Spectroscopy and radiation defects of the $Gd_3Ga_5O_2$ single crystals

Andrii O. Matkovskii[1,2], Dmytro Yu. Sugak[1], Sergii B. Ubizskii[2], Ivan V. Kityk[3]

[1] Research Institute of Materials, RPA "Carat"
202 Stryjska st., Lviv, 290031 Ukraine,
[2] Institute of Physics, HPS
ul. Rejtana 16A, 35-310 Rzeszów, Poland
[3] Institute of Physics, HPS
ul. Armii Krajowej 13/15, 42-201 Częstochowa, Poland

1. Introduction

Many properties of the gadolinium gallium garnets $Gd_3Ga_5O_{12}$ (GGG) single crystals, defining their application in the quantum electronics and microelectronics are notably sensitive to the presence of the point defects and ones induced by the different kinds of the irradiation among them. Particularly an additional optical absorption is induced by the action of the high-energy part of the pumping lamp radiation or γ-quantum, electron and neutron fluxes in the laser hosts fabricated from garnet crystals and causes the rise of the generation threshold and the losses increase at the lasers radiation wavelength [1, 2]. The form of the additional absorption (AA) spectrum (spectral range, the number of lines, their positions, intensity and destruction temperature, lifetimes), and as a consequence the number, the kind and the nature of the colour centers (CC) being connected with them are defined by the set of genetic point defects in the garnet crystals [3, 4]. The latter depends upon the method, regimes and atmosphere of crystal growth, the raw materials purity (the kind and concentration of uncontrolled impurities and the presence of the activators) and from after growing treatment's conditions.

The studying of the radiation-induced changes of the GGG properties has attracted considerable attention of many investigators [4–11]. However, in spite of the great quantity of publications the appearing data about the formation of the defects and their features are very often in contradiction with themselves. This is mainly caused by the complexity of the crystal chemical structure of the garnet, by different physical processes taking part during the irradiation of crystals (recharging of the growing defects, creation of the defects after the impact mechanism, radiation induced disordering) and also by the variety of possible defects configurations, only some of which being considered usually. Moreover, there are practically no theoretical investigations of the defects configuration in these crystals being able to clear in great part the nature of the observed irradiation-induced properties changes of crystals.

Therefore in the present work an attempt to generalize the results of the radiation defects investigations in GGG crystals obtained by the authors within the recent ten years (as well as ones given in publications) is done. They include the experimental investigations of the influence of different kinds of the ionizing radiation on the spectral-luminescent and photoelectrical properties of the GGG crystals and the theoretical studies using quantum-chemical calculation of some characteristics of defects and phenomenological modelling of their formation processes.

2. Samples and investigation methods

The GGG single crystals were grown by the Czochralski method from the iridium crucible in the weak-oxidizing atmosphere. The fragment of the GGG crystal structure is shown in Fig. 1 [12]. During the growth the crystal's content deviates from the stoichiometrical one (the Gd_2O_3 excess is equal to 1.15 mol. %). The nonstoichiometry of the content is the source of the creation the genetical (growing) point defects: the octahedrally coordinated gadolinium ions (the main position of Gd^{3+} in the GGG structure is dodecahedron) in the quantity 0.03–0.05 per formula, and the vacancies in the oxygen and gallium sublattices, the concentration of which can reach 10^{19} cm^{-3} [13, 14].

The concentration of the uncontrolled impurities did not exceed 10^{-3} wt.%. Coming out from the X-ray luminescence data ions of Tb, Eu, Sm, Cr in the concentrations of the order 10^{-4} wt.% are present in the formally pure GGG samples [15]. The contents of the calcium ions being specially introduced into the crystal for the ensurance of the stable growth was less then 10^{-3} wt.%, that did not lead to the change of the optical properties [16]. For the investigation of the impurity influence on the radiation-optical properties of GGG the crystals doped by the different impurities (Mg ($2\cdot10^{-3}$–$6\cdot10^{-3}$ wt.%), Ca (10^{-3}–$2\cdot10^{-2}$ wt.%), Co (10^{-2} wt.%), Fe ($5\cdot10^{-3}$ wt.%), Zr (10^{-2}–10^{-3} wt.%), In (~1 wt.%), Sc (~1 wt.%), Nd (~1 wt.%)) were also investigated. The samples being investigated have been cut in the (111)-plane in the form of the flat-parallel plates with the thicknesses 0.5–5 mm.

Irradiation of the crystals by the g-quanta was performed by the ^{60}Co source with the average energy 1.25 MeV to the absorbed dose 10^2–10^7 Gy. Irradiation by the electrons with the average energy1.3 MeV was done using the electron transformer ELT-1.5 (Institute of the Physical Chemistry of the NAS of Ukraine) without the forced cooling to the absorption dose 10^3–$5\cdot10^7$ Gy. To prevent the heating of samples the irradiation was carried out by the 0.5 s cycles with the next interval of 30 s. The temperature of the samples during the irradiation didn't exceed 330 K. The irradiation by the electrons with the 3.5 MeV energy was performed by the pulse accelerator ELU-4 (Institute of Physics of the NAS of Ukraine) with the forced cooling of the samples by the vapor of the nitrogen up to absorbed doses 10^5–2 108 Gy. Irradiation by the mixed gammaneutron radiation was performed on the research reactor IRT2000 (Institute of the Physics of the Latvian AS) with the fast neutrons flux of $8.5\cdot10^{11}$ cm^{-2} s^{-1} up to fluences 10^{18} cm^{-2} at the temperatures less than 330 K. To cut off thermal and intermediate neutrons the samples were irradiated in the cadmium foil. Irradiation by the protons was performed by the cyclotron MGC-20 (RPA "Positron", St.Petersburg) up to fluences 10^{14} cm^{-2}. The energy of the particles was equal to 12 MeV. Irradiation by the ions of the neon was carried out on the "Vesuvius"-installation up to fluences 10^{13}–$2\cdot10^{15}$ cm.

The absorption spectra were registrated by the spectrophotometer "Specord-M40". The value of the AA was determined as $\Delta K = (1/d)\cdot\ln(T_1/T_2)$, where d is the thickness of the sample, T_1 and T_2 are optical transition before and after the irradiation. For the samples irradiated by the ions an additional optical density $\Delta D = \lg(T_1/T_2)$ was measured because the thickness of the implanted layer was about 0.1 μm.

The temperature dependences of the optical and electrophysical properties were obtained using the special unit, having allowed to change the temperature within the 300...700 K and

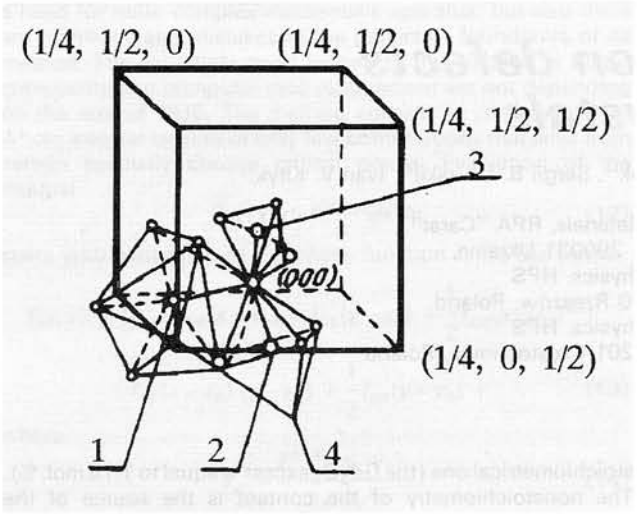

Fig. 1. A part of GGG single crystal structure, 1 – dodecahedral, 2 – octahedral, 3 – tetrahedral lattice assemblies; 4 – oxygen ions

to ensure the linearity and stability of the heating. The thermo-stimulated conductivity (TSC) and thermoglow (TG) were measured by the linear heating rate 0.2 K/s. The luminescence, luminescence excitation and photoconductivity spectra measurements were performed on an equipment based on the monochromator SF-4A.

Investigation of the transient CC was performed using the excitation of the crystals by the single pulses of the highcurrent accelerator of the electrons GIN-600 (Institute of the Physics of the Latvian AS). The pulse duration was equal to 5 μs at the electron energy of 300 keV and at the current density of 100 A/cm^2. The transient absorption spectra were measured in the spectral range 30000–15000 cm^{-1} at the time of the pilot pulse of 50 μs [17].

3. Experimental results

3.1. Spectral properties

The X-ray photo-electron spectrum reflecting the electrons states density of the GGG crystals is presented in Fig. 2. The first band is caused by photo-emission of 4f-electrons of Gd^{3+}. The second one has two maxima at 9.1 and 9.7 eV, which probably correspond to the emission both of own 2p-electrons of oxygen and of the electrons building up the 2p-shell and genetically connected with Ga ions. Their states form the top of the valence band of the crystal. The genetical tie of electrons building up the 2p-shell of oxygen with the cations can be caused by the existence of the covalent component of the chemical bond in GGG [18]. The band of 4f-states of Gd^{3+} is placed rather near to the top of the valence band and is probably partially overlapped in energy with the valence band states. The third wide band with the clearly resolved structure is placed further in the high energy region and is formed by the 5p-Gd (19 eV), 3d-Ga (20.5 eV) and 2s-O (23.6 eV) states. The maximum of the photoemission of electrons forming the 5s-shell of Gd^{3+} occurs near to 42 eV.

The absorption of the GGG in UV-range ($\nu > 50000$ cm^{-1}) reaches 10^5 cm^{-1} and more, and the reflection spectra in this range are characterized by the group of the maxima at 12.2, 10.2, 9.25, 8.2, 6.85 and 5.8 eV. Because the energy interval between the first and second sub-bands of the valence band exceeds 10 eV and the band energy gap of GGG accounts of 5.4 eV the observed peeks can be connected to transitions from the first valence sub-band on the different states of the conduction band, the bottom of which is formed by the 4s-states of the Ga ions placed in the tetrahedral positions.

The absorption edge of GGG is placed in the region 5.4 eV (43550 cm^{-1}) and is related with the direct inter-band transitions. With the increasing of the temperature in the interval

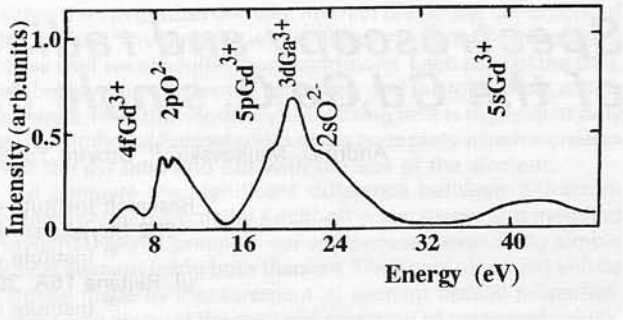

Fig. 2. GGG spectrum of X-ray photoelectrons

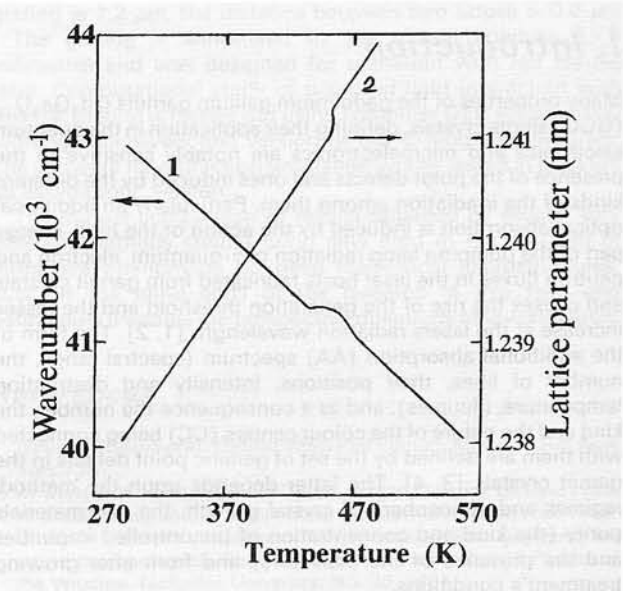

Fig. 3. Temperature dependence of GGG absorption edge position (1) and lattice parameter (2)

$T = 293...443$ K the absorption edge is shifted in the long-wave range by the linear law. The corresponding dependence is shown in Fig. 3 (the wavenumber ν_k, for which the transmission is equal to 20%, was taken to obtain this dependence). But within the range of 443...473 K the leap on the dependences is observed. With the following increase of the temperature the shift has linear dependence too, but the slope angle $\nu_k(T)$ is changed a little. During the repeated heating after the cooling of the crystals the mentioned leap on the dependence $\mu(T)$ is reproduced. The rise of the increment of the lattice constant $a(T)$ (Fig. 3) and the deviation of temperature dependence of the thermal capacity $C_p(T)$ from monotonic one is also observed within the range of 440...470 K. One of the reasons of the leaps occurrence on the dependences $\nu_k(T)$, $\alpha(T)$ and $C_p(T)$ can be the change of the electron shells interaction in GGG during the thermal expansion within 440–550 K.

The narrow intensive bands of the electron intra-center transition in Gd^{3+} ion ($^8S_{7/2} \rightarrow D^6$, ^6P, ^6I) are observed in the optical transmission spectrum in the range 31900...33100, 35600...35500 and 39100...40800 cm^{-1} (Fig. 4) on the background of the weak wide absorption band further in the long-wave range from the absorption edge of GGG. At the $\nu > 32000$ cm^{-1} the crystal is transparent up to the IR absorption edge (1450...1500 cm^{-1}), behind which the absorption bands of the oneand multiphonon vibrations of lattice atoms appear. In the transparency region the absorption coefficient is about ~0.01 cm^{-1}.

The GGG crystal doping of impurities inconcentrations (10^{-3}–10^{-2} wt.%) leads to the slightly decrease of the transparency near the absorption edge (In, Sc, Zr), to the occurrence of the intracenter absorption bands in the trans-

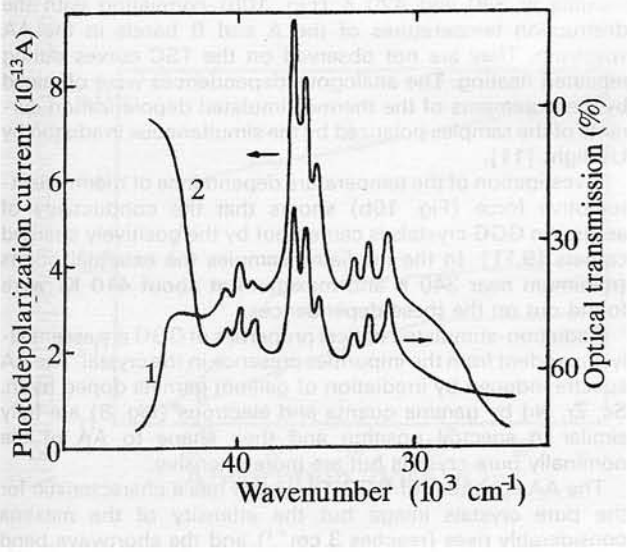

Fig. 4. Spectral dependence of GGG photocurrent (1) and transmission spectrum (2)

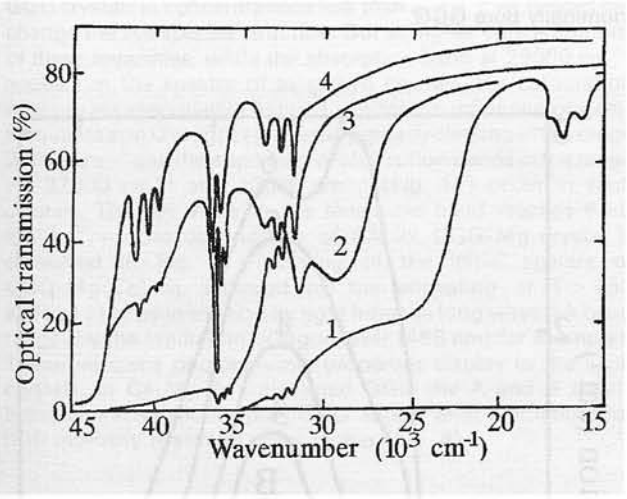

Fig. 5. Transmission spectra of GGG – Co (1), GGG – Mg (2), GGG – Fe (3) and GGG – In (4)

parency region (Nd, Co) and to arising of the wide absorption band with the maximum at the 29000 cm^{-1} (Ca, Mg) (Fig. 5). It is necessary to note that the influence of the Ca^{2+} and Mg^{2+} (Me^{2+}) ions on the optical properties of GGG has the concentration threshold: absorption band at 29000 cm-1 appears in the spectra at the Me^{2+} contents greater than $3 \cdot 10^{-3}$ wt.%. Its intensity increases with rising of the concentration in the range of $(3-7)\ 10^{-3}$ wt.%. With the further increase of concentration up to $2 \cdot 10^{-2}$ wt.% the absorption value accounting of 22 cm^{-2} in the band maximum remains practically unchanged. The doping of the same concentration of Zr^{4+} together with the two-valence impurity leads to the disappearance of the band at 29000 cm^{-1}. One can presume that the AA at 29000 cm^{-1} is caused by the creation of the stabilized complex colour centers (CCC) $[Me^{2+}F^{+}]$ formed by two-valence impurity ion and oxygen vacancy (V_0) with one electron localized near it and compensating the relative negative charge excess of impurity. The charge caused by impurity doping is compensated in Ca-Mg-Zr-substituted GGG that prevents the creation of both the significant number of V_0 and CCC. Sometimes during the growth of GGG crystals containing Ca in the concentration more than $3 \cdot 10^{-3}$ wt.% due to the fluctuation of the temperature gradient the aggregates of the point defects $[Me^{2+}F^{+}]$ can arise being observed on the etched surfaces of

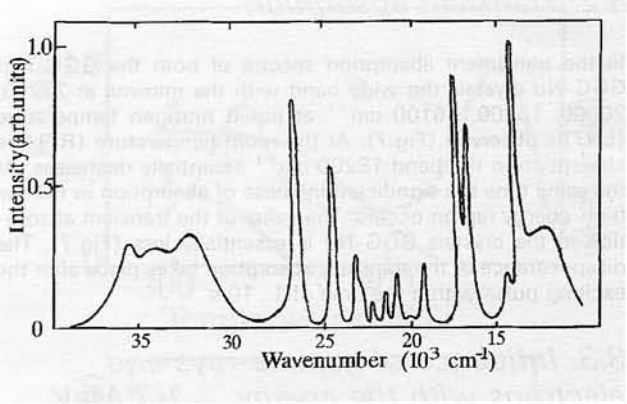

Fig. 6. GGG X-ray luminescence spectrum

the polished crystal plates in the form of the concentric ring-like areas [4].

The appearance of the ions Fe^{3+} in the crystals is accompanied by the essential decrease of the material transparency in the UV-range (up to 31000 cm^{-1}) due to the superposition of the intensive band of charge transfer $O^{2-} \rightarrow Fe^{3+}$ on the absorption edge. The wide band with the maximum at 12650 cm^{-1} arises in the luminescent spectra too which is caused by the $^4T_1(G) \rightarrow {}^6A_1(S)$ transitions of the tetrahedral Fe^{3+} ions.

At the simultaneous action of the electrical field and of the light of the range 40000 – 25000 cm^{-1} the photoelectrete state in the crystals GGG is formed. During the next irradiation by the light the photodepolarization current appears. The spectral dependence of the photodepolarized current in the GGG crystals is characterized by the weak band in the range of interband transitions (44500...42000 cm^{-1}) and by the wide one within 42000...25000 cm^{-1}. On the background of the last the set of the narrow intensive lines is observed (Fig. 4). They are coincident by the spectral positions with the maxima of the *f-f*-transitions in the absorption spectrum and corresponding to the carriers photogeneration due to exciting of the Gd^{3+} ion.

The presence of the weak absorption and of the wide photogeneration band within 42000 – 25000 cm^{-1} indicates the existence of the folled electronic states formed by the defects of the oxygen sublattices and by the impurities in the band energy gap.

"Unusual" carriers photogeneration during light absorption by the Gd^{3+} ions is realized by transmission of the exciting energy from Gd to defect centers with the following their ionization. According to the proposed mechanism the energy transmission can take place both by non-radiative way and by one of the reabsorption of the energy of the excited gadolinium by defect centers (the weak luminescence of the Gd^{3+} ions is observed in the luminescent spectra of GGG [15]). Therefore the photocurrent intensity is very sensitive to the changes of the defect subsystem of the crystal. Particularly, by the GGG doping of the Me^{2+} ions in the concentrations higher than threshold the practically fully suppression of the photosensitivity in the range 42000 – 25000 cm^{-1} happens. This is caused by the bounding of the oxygen defects (which could be the electrons suppliers) into CCC having the basic and excited states in the energy gap of crystal.

During excitation of GGG by the electronic beam or by the X-ray quanta the wide band of the own luminescence with maximum at 33800 cm^{-1} takes place (Fig.6). On its background two maxima (32000 and 35650 cm^{-1}) of the luminescence of Gd^{3+} ions (transitions ^6P and $^6I \rightarrow {}^8S_{7/2}$) are distinguished. The luminescence of the uncontrolled impurities Tb, Eu, Sm etc. appears in the more long wave range.

The electron excitations localized on the genetic defects (for example Gd^{3+} in the octahedral positions trapped a hole) occur in GGG crystals as well as in the crystals of $Y_3Al_5O_{12}$ [19]. A part of them recombines what is accompanied by luminescence with maximum at 33800 cm^{-1}, and the others can take part in the colour centers formation.

3.2. Transient absorption

In the transinient absorption spectra of both the GGG and GGG-Nd crystals the wide band with the maxima at 23200, 20000, 18200, 16100 cm^{-1} at liquid nitrogen temperature (LNT)is observed (Fig.7). At the room temperature (RT) the absorption in the band 18200 cm^{-1} essentially decreases. At the same time the significant increase of absorption in the the high-energy region occurs. The value of the transient absorption in the crystals GGG-Nd is essentially less (Fig.7). The disappearance of the transient absorption takes place after the exciting pulse within the time of 1...10 s.

3.3. Influence of gamma-rays and electrons with the energy ~1.3 MeV

In the irradiated by the γ-quanta ($E^{\sim}$1.25 MeV) and electrons ($E^{\sim}$1.3 MeV) crystals GGG the wide band of AA in the region 34000 – 11000 cm^{-1} and the clearing near the absorption edge occur at the absorption doses $10^2 - 10^7$ Gy. The spectra of AA being characteristic for GGG crystals irradiated in the above mentioned regimes are shown on Fig. 8. The analogous in spectral position and in the structure AA appears in GGG irradiated by the X-ray quanta and by the more low-energy electrons (for example at the $E = 0.3$ MeV). The spectrum of AA consists from at least two overlapping bands with maxima in the region 32000 – 29000 cm^{-1} (band A) and 24000 – 21000 cm^{-1} (band B). The division of AA on two bands is in some sense ambiguous because one can't exclude that its spectrum has more complicated structure. The value of AA increases with the irradiation dose and in the region of $10^4 - 10^6$ Gy its saturation takes place (Fig.9). The maximal value of the induced absorption in GGG does not exceed 1 cm^{-1}.

The preliminary annealing at 900 K in the different media (air, inert atmospheres) leads to the change of the relative intensity of the A- and B-bands and the degree of clearing of irradiated crystals.

In Fig. 10 the curves of the annealing of the A- and B-bands of AA are presented. The short-wave band disappears at the temperatures about 340 K and the long-wave one at 410 K. Destruction of A band leads to the a slight decrease of clearing while during the B-band destruction the clearing disappears completely.

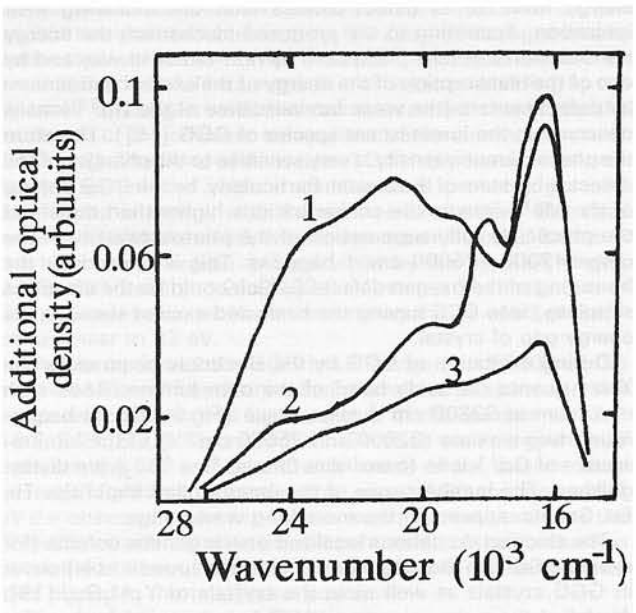

Fig. 7. Transient absorption spectra of GGG (1, 2) and GGG – Nd (3) at 300 (1) and 77 K (2, 3)

The curves of TSC of irradiated GGG samples have two maxima at 340 and 420 K (Fig. 10b) correlating with the destruction temperatures of the A and B bands in the AA spectrum. They are not observed on the TSC curves during repeated heating. The analogous dependences were obtained by measurements of the thermostimulated depolarization currents of the samples polarized by the simultaneous irradiaton by UV light [11].

Investigation of the temperature dependence of thermoelectromotive force (Fig. 10b) shows that the conductivity of as-grown GGG crystals is carried out by the positively charged carriers [9,11]. In the irradiated samples the extremal points (minimum near 340 K and maximum at about 410 K) were found out on the these dependences.

Radiation-stimulated optical properties of GGG are essentially dependent from the impurities presence in the crystal. The AA spectra induced by irradiation of gallium garnets doped by In, Sc, Zr, Nd by gamma quanta and electrons (Fig. 8) are fully similar in spectral position and their shape to AA of the nominally pure crystals but are more intensive.

The AA spectrum of GGG-Fe crystal has a characteristic for the pure crystals image but the intensity of the maxima considerably rises (reaches 3 cm^{-1}) and the shortwave band A becomes dominant (Fig.8). Its spectral position is close to the absorption band of the intracenter transitions of Fe^{2+} ions [4].

Probably, changing of the Fe charge occurs in these crystals in parallel with recharging of CC being characteristic for nominally pure GGG.

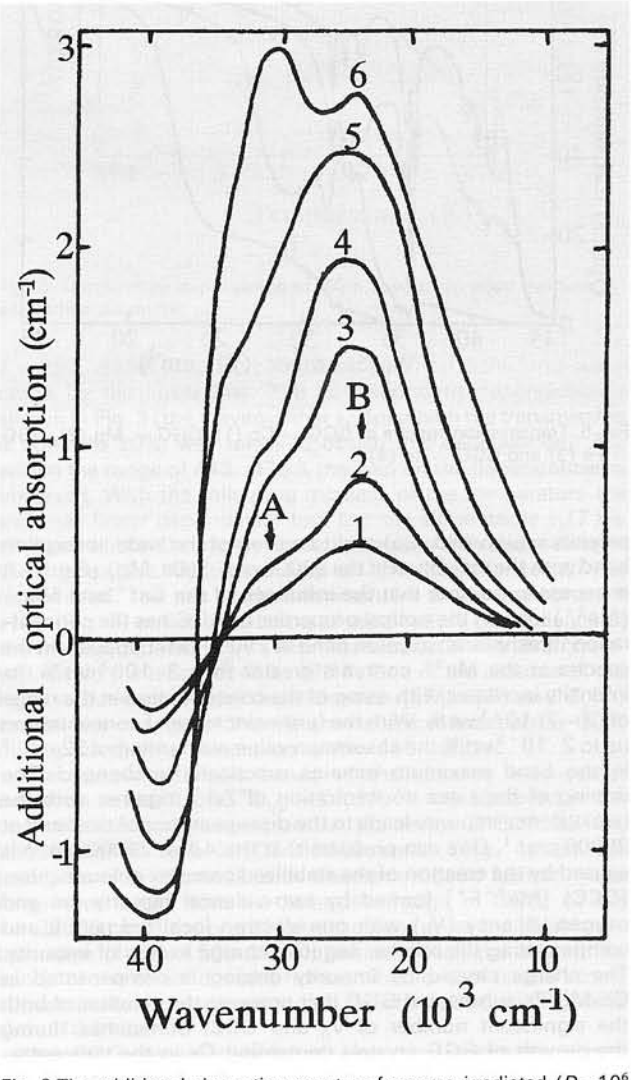

Fig. 8.The additional absorption spectra of gamma-irradiated ($D = 10^6$ Gy) GGG (1), GGG – Nd (2), GGG – Zr (3), GGG – In (4), GGG – Ca-Mg-Zr (5), GGG – Fe (6) crystals

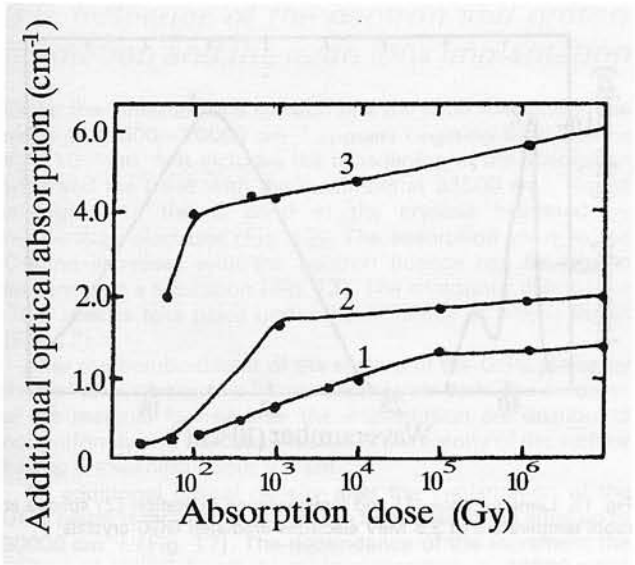

Fig. 9. Dose dependence of AA in 23000 cm^{-1} band gamma-quanta irradiated GGG (1), GGG – In (2), GGG – Mg (3)

The presence of two-valent Ca^{2+} or Mg^{2+} impurities in the GGG crystals in concentrations less than $3 \cdot 10^{-3}$ wt.% does not change the AA spectra structure. But at higher concentrations of these impurities, while the absorption band at 29000 cm^{-1} appears in the spectra of as-grown crystals, the colouration features are essentially changed. Under the influence of gammaquanta and UV-light ([16]) the partially clearing in the range 29000 cm^{-1} and the appearing of absorption bands in the range $\nu > 37000$ cm^{-1} and 23000 cm^{-1} (Fig. 11) occur in such crystals. The AA value in the longwave band reaches 6–8 cm^{-1}. The dose dependence of AA for GGG-Mg crystal is presented in Fig. 9. Restoring of the initial spectra of GGG-Mg(Ca) is achieved by the annealing at $T > 450$ K (Fig.11) or by irradiation by light from the long wave AA band range (by the irradiation of argon laser (488 nm) for example). Therefore some photochromic properties display in the such crystals. In Ca-Mg-Zr substituted GGG the A and B bands being characteristic for pure GGG appear after irradiation but their intensity is several times higher (Fig. 8).

3.4. Influence of electrons with the energies 3.5 MeV

After the irradiation of GGG by electrons with energies 3.5 MeV and fluences of $10^{15}-10^{16}$ cm^{-2} (the absorption dose $D_e = 2 \cdot 10^5 \div 2 \cdot 10^6$ Gy) the wide AA band and clearing near the fundamental edge are observed in the optical absorption spectra. These changes are analogous to that appearing after irradiation by the photons and electrons with the energy 1.3 MeV at doses up to 10^7 Gy. At the fluences $3 \cdot 10^{16}$ cm^{-2} the clearing near the edge disappears and from the fluences $\Phi = 10^{17}$ cm^{-2} ($D_e = 2 \cdot 10^7$ Gy) is changed by the darkening in this range (Fig. 12). Simultaneously on the background of the A and B bands appears a new band of AA with the maximum at 33500 cm^{-1} (the C band). With increasing of the electron fluence up to 10^{18} cm^{-2} the induced absorption value in the maximum of the C band rises up to 15 cm^{-1} and its longwave wing fully overlaps rather weak ($\Delta K < 1$ cm^{-1}) bands A and B. The tendency for a saturation of dose dependence of the absorption in the maximum of the C band is not observed (Fig.13).

On the temperature dependence of the destruction of the C band some regions of different kinetics being characterized by the curve slope change can be distinguished in the vinicity of 330÷340, 400÷420 and 500÷600 K (Fig. 14). The first two temperature regions correlate well with the temperatures of the destruc tion of the A and B bands (Fig.10). The disappearence of the C band takes place at $T > 620$ K but the broadening of the

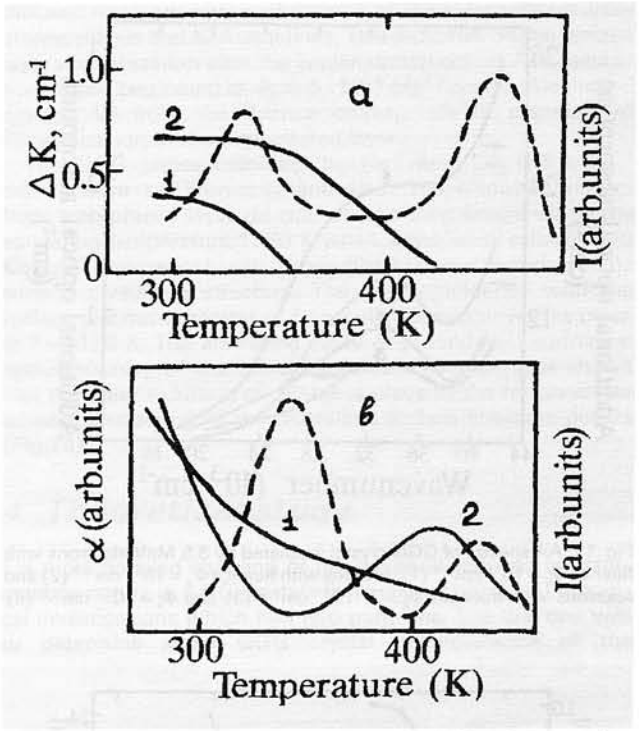

Fig. 10. Thermodestruction of AA bands A(1), B(2) and thermoglow curve (---) of gamma-quanta irradiated GGG (a); Temperature dependence of thermoelectromotive force before (1) and after (2) gamma-irradiation (b); (---) thermostimulated current (TSC) of gamma irradiated GGG

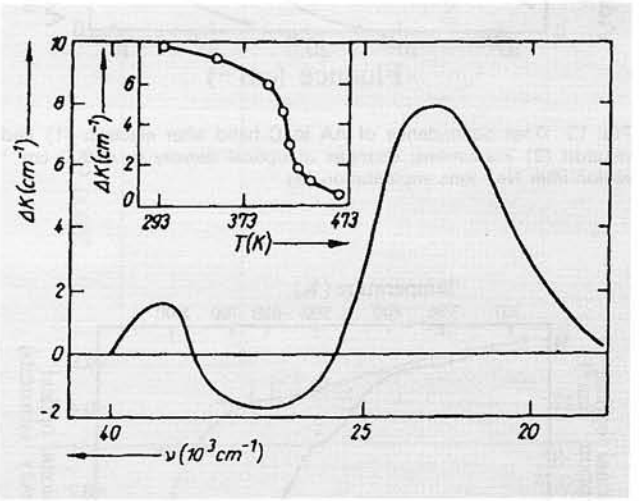

Fig. 11. AA spectrum in $Gd_3Ga_5O_{12}-Me^{2+}$ crystals caused by laser light irradiation ($\lambda = 337$ nm). Insert: Thermodestruction of the AA band with maximum 23000 cm^{-1}

fundamental edge partially is preserved. The full restoring of the GGG spectrum occurs after the annealing at $T > 1000$ K.

In the X-ray luminescence spectra of GGG irradiated by the high-energy electrons the intensity of uncontrolled impurities luminescence of rare-earth and transitional metals being characteristic for the as-grown crystals decreases and a new wide band occurs with the maximuma at about 19000 cm^{-1} at RT (Fig.15). The analogous luminescence band is observed in GGG crystals annealed in reducton atmosphere. It should be noted that this band does not appear in the crystals irradiated by electrons at doses less than 10^7 Gy.

The luminescence excitation spectrum in the region 19000 cm^{-1} is shown in Fig. 15 too. The luminescence is excited most efficiently in the vicinity of the absorption edge and in the bands corresponding to the intracenter transitions of Gd^{3+} ions

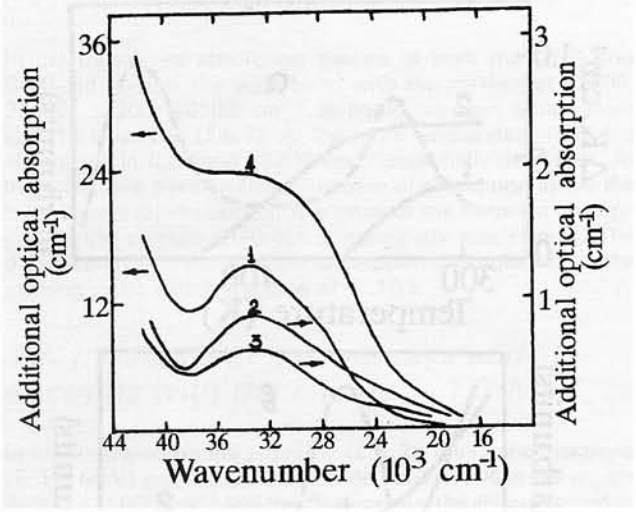

Fig. 12. AA spectra of GGG crystal irradiated by 3.5 MeV electrons with fluence $\Phi_e = 10^{18}$ cm^{-1} (1); protons with fluence $\Phi_p = 10^{14}$ cm^{-2} (2) and neutrons with fluences $\Phi_n = 2 * 10^{15}$ cm^{-2} (3) and $\Phi_n = 10^{17}$ cm^{-2} (4)

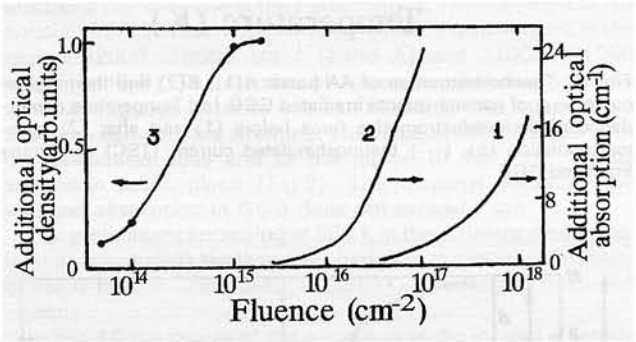

Fig. 13. Dose dependence of AA in C-band after electron (1) and neutron (2) irradiations; changes of optical density in 42000 cm^{-1} region after Ne^+ ions implantation (3)

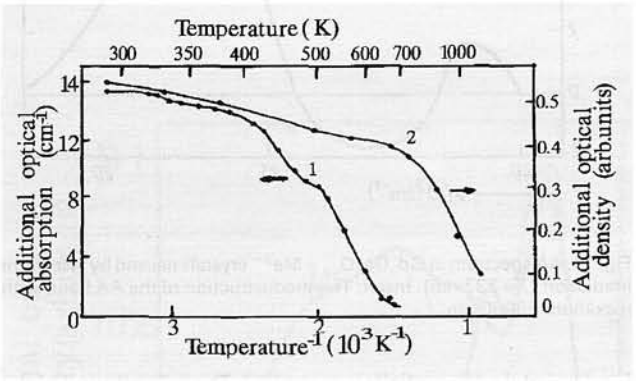

Fig. 14. Thermodestruction of the AA in 33500 cm^{-1} band (1) and 42000 cm^{-1} (2). 1 – crystals irradiated by electrons ($E = 3.5$ MeV, $\Phi_e = 10^{18}$ cm^{-2}); 2 – crystals irradiated by Ne^+ ions

(40000÷32000 cm^{-1}). The intensity of luminescence at 19000 cm^{-1} of the irradiated GGG crystals increases with the temperature rise from 90 K reaching maximal value at 210÷220 K (Fig. 16). At the higher temperatures the intensity of luminescence falls down to its full putting out at 400 K.

An increasing of X-ray luminescence 19000 cm^{-1} of the annealed crystals with the temperature rise starts at T > 200 K where the luminescence intensity of the irradiated crystals

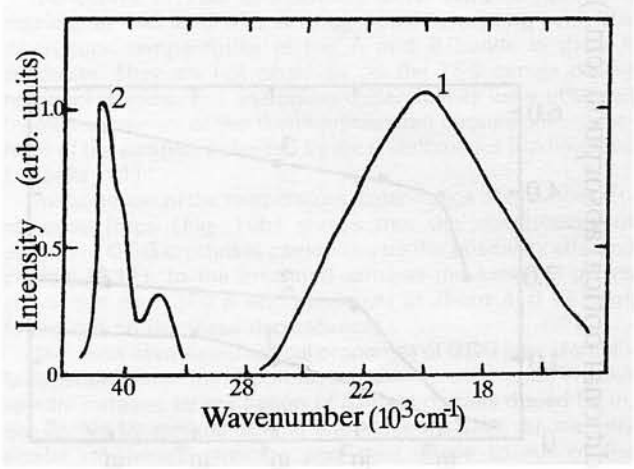

Fig. 15. Luminescence (1) and luminescence excitation (2) spectra at room temperature of 3.5 MeV electrons irradiated GGG crystals

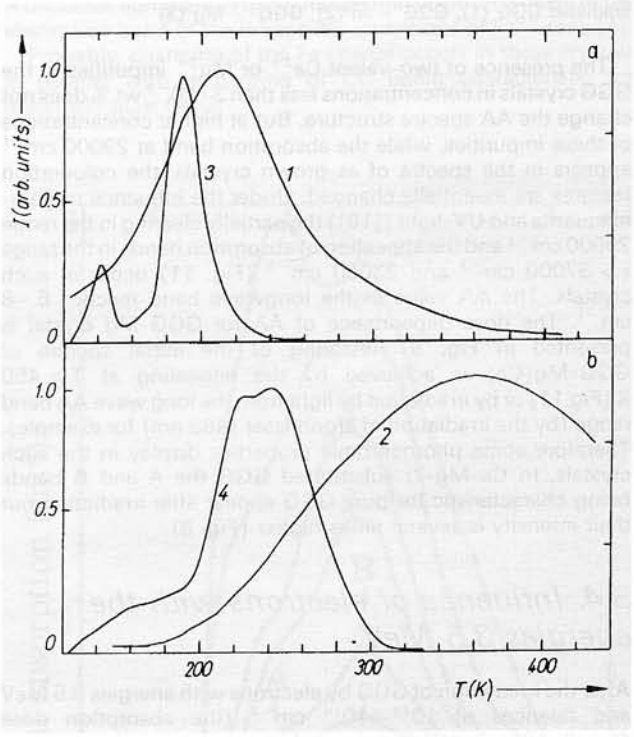

Fig.16 Temperature dependence of luminescence output in the 19000 cm^{-1} band (1, 2) for a) irradiated or b) reduced GGG crystals after Ne^+ ions implantation by $5 \cdot 10^{-14}$ cm^{-2} fluence

reaches its maximum value. An appreciable temperature extinguishing of luminescence in the annealed crystals was not observed up to temperatures 500÷550 K.

The curves of thermo-glow (TG) in the band of 19000 cm^{-1} of the irradiated (curve 3) and annealed (curve 4) GGG crystals after excitation by X-ray irradiation at LNT are presented in Fig. 16 too. On the TG curve of the irradiated GGG crystal the intensive maxima at 130 and 190 K and low intensive ones being displayed in form of the curve bends at 160 and 210 K are observed. The TG of the annealed crystal occurs in the wide temperature range spreaded from 100 to 300 K on with maxima at 220 and 245 K being able to be distinguished on its background.

Irradiation of the GGG crystals by the high-energy electrons with the fluence up to 10^{18} cm^{-2} leads also to the rise of the specific resistivity and to the reduction of the current output in 3÷5 times.

3.5. Influence of the neutron and proton irradiation and the neon ions implantation

Under the influence of a neutron flux the wide AA band in the range of 43500÷20000 cm^{-1} appears begining from fluence $\Phi_n = 10^{15}$ cm^{-2}. It includes the broadening of the absorption edge and the band with the maximum at 33500 cm^{-1} being analogous to the C band in the crystals irradiated by high-energy electrons (Fig. 12). The absorption value in the C band increases with the neutron fluence rise having no tendency for a saturation (Fig. 13). The analogous changes in GGG spectra take place under the influence of proton fluxes (Fig. 12).

After the bombardment of the surface of the GGG plates by the Ne^+ ions the samples became appreciabl dark. The damages of the material formed after the implantation are distributed nonuniformly and are concentrated in the visinity of the surface having a thickness about 0.1 μm.

An additional optical density after the implantation of the GGG plates is induced in the region from absorption edge up to 30000 cm^{-1} (Fig. 17). The dependence of the increment the additional optical density for the wavenumber $\nu = 42000$ cm^{-1} as the function of the ion fluence is presented in Fig. 13.

On the electronogramms of surface of GGG irradiated by the Ne^+ ions with fluences higher than $6 \cdot 10^{14}$ cm^{-2} only the diffused rings are observed instead of the clear reflexes from atomic planes and Kickuchi lines. This indicates on the surface layer amorphization after the implanatation occurs. The saturation region beginning at $\Phi_1 > 5 \cdot 10^{14}$ cm^{-2} on the dependences of ΔD from the fluence corresponds to occuring of amorphization in the implantated layer.

The GGG plates irradiated by Ne^+ ions ($\Phi_1 = 1.8 \cdot 10^{15}$ cm^{-2}) were isochronically annealed. The electronogramms from amorphized layer do not change their image up to the annealing temperature 1070 K when some weak reflexes and Kickuchi-lines were found. This indicates partial restoring of the surface crystalline structure. The full coincidence with the surface electronogramms of non-radiated samples takes place at $T = 1170$ K. The annealing curve of the induced additional optical density of the same implanted GGG samples shows that the main reducing of ΔD takes place at the temperatures when the restoring of the crystalline surface structure occurs (Fig.14).

4. Theoretical study

For more detailed studying of the radiation-induced transformations nature in GGG crystals there were performed theoretical investigations which had two purposes. The first one was to determine some GGG crystal characteristics of the

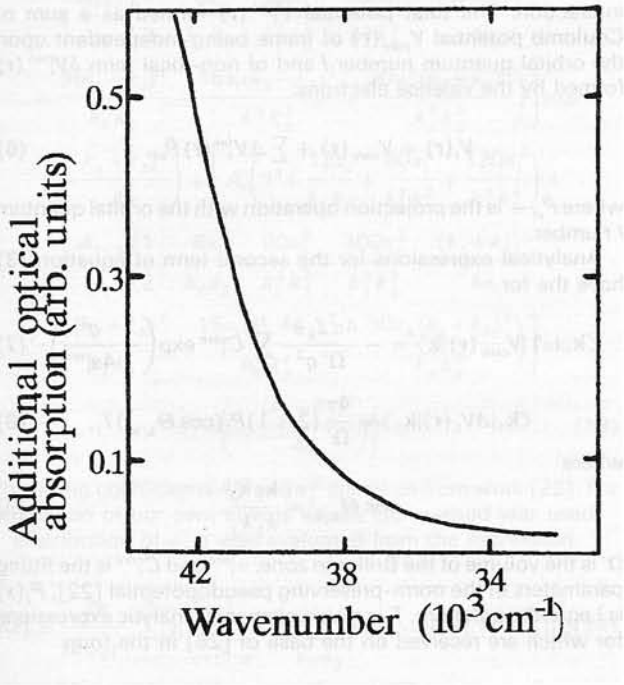

Fig. 17. Induced optical density spectrum of GGG crystals after Ne^+ ions implatation by $5 \cdot 10^{-14}$ cm^{-2} fluence

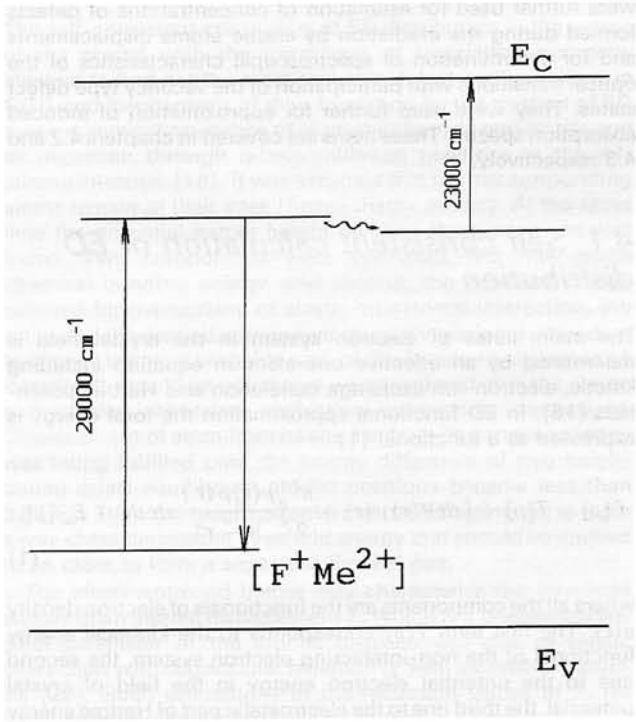

Fig. 19. Energy levels of defects in GGG Me^{2+}

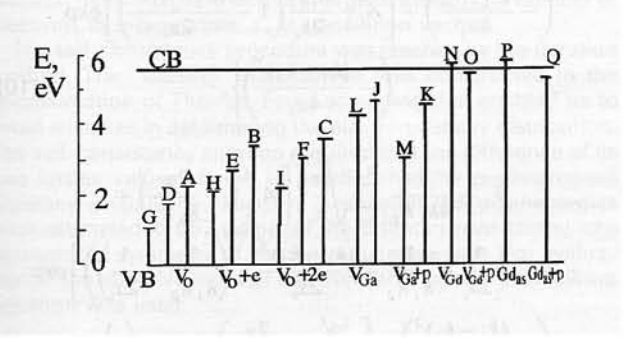

Fig. 18. Scheme of energetic levels of GGG with the vecancy type defects

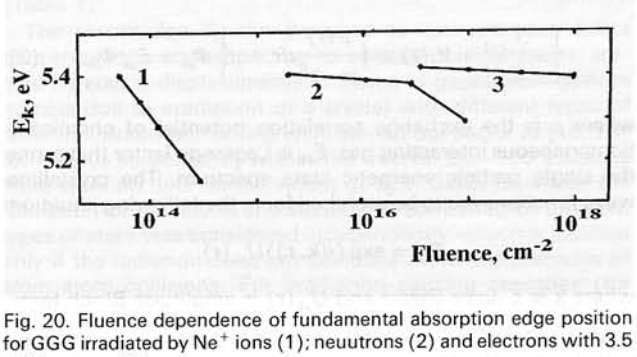

Fig. 20. Fluence dependence of fundamental absorption edge position for GGG irradiated by Ne^+ ions (1); neuutrons (2) and electrons with 3.5 MeV energy (3)

both the ideal structure and including structure defects on the base of solution of the task of the self-consistent calculation of electron charge density distribution. The second purpose was to make an attempt of interpretation of the experimental data with the use of phenomenological models with the results of quantum-chemical calculations being used as their parameters. For solution of the first task there was used the method of non-local normpreserving pseudopotential that is fruitfully used in calculations of band energies of the structurally ideal crystals of semiconductors and dielectrics [20]. At the first stage calculations of space distribution of an ideal crystal electron charge in the state of minimal functional of electron density (ED) were fulfilled. Data on atom coordinates in GGG crystal structure [21] and the pseudopotentials from the work [22] were used as the initial data. The calculations enabled us to find such basic characteristics as chemical bond energies, degree of their ionicyty, ion radii, etc. The method of self consistent calculation of ED will be described further in chapter 4.1. At the second stage the calculations were done with the account of translational symmetry crystal distortions caused by defect states in the crystals. As the result there were determined energetic levels of single defects, the most probable directions of the crystal atoms' shifts during formation of the defects in lattice sites of GGG and the threshold energy values that are necessary for displacements, effective charges, unstability zone radii (annihilation radii) and the defect centers migration energies.

The data, obtained from the above mentioned calculations, were further used for estimation of concentrations of defects formed during the irradiation by elastic atoms displacements and for determination of spectroscopic characteristics of the optical transitions with participation of the vacancy type defect states. They were used further for approximation of induced absorption spectra. These items are covered in chapters 4.2 and 4.3 respectively.

4.1. Self consistent calculation of ED distribution

The main states of electron system in the crystal field is determined by an effective one-electron equation including kinetic, electron-ion exchange correlation and Hartree potentials [18]. In ED functional approximation the total energy is expressed as a functional (1)

$$E[\rho] = T[\rho] + \int d\mathbf{r} V(\mathbf{r})\rho(\mathbf{r}) + \frac{e^2}{2}\int \frac{\rho(\mathbf{r})\rho(\mathbf{r}')}{|\mathbf{r}-\mathbf{r}'|} d\mathbf{r}\, d\mathbf{r}' + E_{xc}[\rho], \tag{1}$$

where all the components are the functionals of electron density $\rho(\mathbf{r})$. The first term $T(\rho)$ corresponds to the kinetical energy functional of the non-interacting electron system, the second one to the potential electron energy in the field of crystal potential, the third one to the electrostatic part of Hartree energy and the last one to the exchange correlation energy.

According to [23] the solution of equation (1) may be done by a self consistent solution of the Schrödinger equation system:

$$\left\{-\frac{1}{2}\nabla^2 + V_i(\mathbf{r}) + \int \frac{\rho(\mathbf{r})}{|\mathbf{r}-\mathbf{r}'|} d\mathbf{r} + \mu\right\} \Phi_{nk} = E_{nk}\Phi_{nk}, \tag{2}$$

where μ is the exchange correlation potential of chemically homogeneous interacting gas, E_{nk} is Lagrange factor that forms the single particle energetic state spectrum. The crystalline wave functions are to be searched for in the following equation

$$\Phi_{nk} = \exp(i(\mathbf{k},\mathbf{r}))U_{nk}(\mathbf{r}),$$

where $\mathbf{k}$ is a wave vector and $U_{nk}(\mathbf{r})$ is amplitude Bloch term.

Matrix elements of singular equation in a plane wave basis are calculated in the form;

$$\langle \mathbf{k}_1|\hat{H}|\mathbf{k}_2\rangle = \frac{k_i^2}{2}\delta_{\mathbf{k}1+\mathbf{k}2} + \sum_{\alpha} S^{\alpha}(\mathbf{q})V_i^{\alpha}(\mathbf{k}_1,\mathbf{k}_2) + \frac{4\pi}{|\mathbf{q}|^2}\rho(\mathbf{q}) +$$

$$+ \int d\mathbf{r} \exp(i\mathbf{q}\mathbf{r})\mu_{xc}(\rho), \tag{3}$$

where $\mathbf{k}_1 = \mathbf{k} + G_i$, $\mathbf{k}_2 = \mathbf{k} + G_j$, $\mathbf{q} = G_i - G_j$, $S^{\alpha}(\mathbf{q})$ is atom structure factor of α-type and G_m are vectors of the reverse lattice. Contribution of Coulomb and exchange-correlation potential is obtained analytically after the Fourier transforms into the reverse space. For estimation of the exchange-correlation potential two equations parameterized in [24] were used. These equation depending upon the electron concentration may have the forms

$$\mu_{xc} = \begin{cases} -\dfrac{0.6193}{r_s} - \dfrac{0.1432}{1+1.0529\sqrt{r_s}+0.3334r_s} \times \\ \times\left[1 + \dfrac{0.5264\sqrt{r_s}+0.3334r_s}{3(1+1.0529\sqrt{r_s}+0.3334r_s}\right], \; r_s > 1 \quad (4) \\ -\dfrac{0.6193}{r_s} + 0.031\cdot\ln(r_s) - 0.0583, \; r_s < 1, \quad (5) \end{cases}$$

where $r_s = (3/(4\pi\rho)^{1/3}$ and the first term corresponds to the exchange potential in the form of Gaspar-Kohn-Sham [25].

The calculation scheme takes into account the relativistic corrections. The ionic potential $V_i(\mathbf{r})$ is averaged by j and l quantum numbers and takes into account the spin-orbital interaction. The total potential $V_i^{(im)}(\mathbf{r})$ formed as a sum of Coulomb potential $V_{core}(\mathbf{r})$ of frame being independent upon the orbital quantum number l and of non-local term $\delta V_i^{(im)}(\mathbf{r})$ formed by the valence electrons:

$$V_i(\mathbf{r}) = V_{core}(\mathbf{r}) + \sum_l \Delta V_l^{ion}(\mathbf{r})\hat{P}_{rl}, \tag{6}$$

where $\hat{P}_{rl}$ – is the projection operation with the orbital quantum l number.

Analytical expressions for the second term of equation (3) have the for

$$\langle \mathbf{k}+\mathbf{1}|V_{core}(\mathbf{r})|\mathbf{k}\rangle = -\frac{4\pi Z_v e^2}{\Omega' q^2}\sum_{i=1}^{2} C_i^{core}\exp\left(-\frac{q^2}{4\alpha_i^{core}}\right), \tag{7}$$

$$\langle \mathbf{k}_1|\Delta V_l(\mathbf{r})|\mathbf{k}_2\rangle = \frac{4\pi}{\Omega'}(2l+1)P_l(\cos\Theta_{\mathbf{k}_1\mathbf{k}_2})T_l, \tag{8}$$

where

$$\cos\Theta_{\mathbf{k}_1\mathbf{k}_2} = \frac{\mathbf{k}_1\mathbf{k}_2}{k_1 k_2}, \tag{9}$$

Ω' is the volume of the Brillouin zone, α_i^{core} and C_i^{core} is the fitting parameters of the norm-preserving pseudopotential [22], $P_l(x)$ is Legandre polynom, T_l is matrix elements, analytic expressions for which are received on the base of [26] in the form

$$T_0 = \frac{1}{4k_1k_2}\sum_{i=1}^{3}\sqrt{\frac{\pi}{\alpha_i}}\left\{\left[A_i + \frac{A_{i+3}}{2\alpha_1}\left(1 - \frac{(k_1-k_2)^2}{2\alpha_i}\right)\right]\exp\left(-\frac{(k_1-k_2}{4\alpha_1}\right) - \left[A_i + \frac{A_{i+3}}{2\alpha_i}\left(1 - \frac{(k_1+k_2)^2}{2\alpha_i}\right)\right]\exp\left(-\frac{(k_1+k_2)^2}{4\alpha_1}\right)\right\}, \tag{10}$$

$$T_1 = \frac{1}{4k_1k_2}\sum_{i=1}^{3}\sqrt{\frac{\pi}{\alpha_i}}\left\{\left[A_i\left(1 - \frac{2\alpha_i}{k_1k_2}\right) + A_{i+3}\left(\frac{1}{2\alpha_i} + \frac{1}{k_1k_2} + \frac{(k_1-k_2)^2}{2\alpha_i}\times\left(\frac{1}{k_1k_2} - \frac{1}{2\alpha_i}\right)\right)\right]\exp\left(-\frac{(k_1-k_2)^2}{4\alpha_1}\right) + \left[A_i\left(1 + \frac{2\alpha_1}{k_1k_2}\right) + A_{i+3}\left(\frac{1}{2\alpha_i} -\right.\right.$$

$$-\frac{1}{k_1 k_2}-\frac{(k_1+k_2)^2}{2\alpha_i}\left(\frac{1}{k_1 k_2}+\frac{1}{2\alpha_i}\right)\Bigg)\Bigg]\exp\left(-\frac{k_1+k_2)^2}{4\alpha_i}\right)\Bigg\}, \quad (11)$$

$$T_2=\frac{1}{4k_1k_2}\sum_{i=1}^{3}\sqrt{\frac{\pi}{\alpha_i}}\Bigg\{\Bigg[A_i\left(\frac{12\alpha_i^2}{k_1^2k_2^2}-\frac{6\alpha_i}{k_1k_2}+1\right)+$$
$$+A_{i+3}\left(\frac{1}{2\alpha_i}+\frac{3}{k_1k_2}-\frac{18\alpha_1}{k_1^2k_2^2}-\frac{3(k_1-k_2)^2}{k_1^2k_2^2}-\right.$$
$$\left.-\frac{(k_1-k_2)^2}{4\alpha_i}+\frac{3(k_1-k_2)^2}{2\alpha_i k_1k_2}\right)\Bigg]\exp\left(-\frac{(k_1-k_2)^2}{4\alpha_i}\right)+$$
$$+\Bigg[A_i\left(-\frac{12\alpha_i^2}{k_1^2k_2^2}-\frac{6\alpha_i}{k_1k_2}-1\right)+A_{i+3}\left(-\frac{1}{2\alpha_i}+\frac{3}{k_1k_2}+\frac{18\alpha_1}{k_1^2k_2^2}+$$
$$+\frac{3(k_1+k_2)^2}{k_1^2k_2^2}+\frac{(k_1+k_2)^2}{4\alpha_i}+\frac{3(k_1+k_2)^2}{2\alpha_i k_1k_2}\right)\Bigg]\exp$$
$$\left(-\frac{(k_1+k_2)^2}{4\alpha_i}\right)\Bigg\}, \quad (12)$$

$$T_3=\frac{1}{4k_1k_2}\sum_{i=1}^{3}\sqrt{\frac{\pi}{\alpha_i}}\Bigg\{\Bigg[A_i\left(1-\frac{12\alpha_i}{k_1k_2}+\frac{60\alpha_i^3}{k_1^2k_2^2}-\frac{120\alpha_i^3}{k_1^3k_2^3}\right)+$$
$$+\frac{A_{i+3}}{\alpha_i}\left(\frac{1}{2}+\frac{6\alpha_i}{k_1k_2}-\frac{90\alpha_i^2}{k_1^2k_2^2}+\frac{300\alpha_i^3}{k_1^3k_2^3}-\frac{(k_1-k_2)^2}{4\alpha_i}+\right.$$
$$\left.+\frac{3(k_1-k_2)^2}{k_1k_2}-\frac{15\alpha_i(k_1-k_2)^2}{k_1^2k_2^2}+\frac{30\alpha_i^2(k_1+k_2)^2}{k_1^3k_2^3}\right)\Bigg]\exp$$
$$\left(-\frac{k_1+k_2)^2}{4\alpha_i}\right)+\Bigg[A_i\left(1+\frac{12\alpha_i}{k_1k_2}+\frac{60\alpha_i^2}{k_1^2k_2^2}+\frac{120\alpha_i^3}{k_1^3k_2^3}\right)+$$
$$+\frac{A_{i+3}}{\alpha_i}\left(\frac{1}{2}-\frac{6\alpha_i}{k_1k_2}-\frac{90\alpha_i^2}{k_1^2k_2^2}-\frac{300\alpha_i^3}{k_1^3k_2^3}-\frac{(k_1+k_2)^2}{4\alpha_i}-\right.$$
$$\left.-\frac{3(k_1+k_2)^2}{k_1k_2}-\frac{15\alpha_i(k_1+k_2)^2}{k_1^2k_2^2}-\frac{30\alpha_g(k_1+k_2)^2}{k_1^3k_2^3}\right)\Bigg]\exp$$
$$\left(-\frac{(k_1+k_2)^2}{4\alpha_i}\right)\Bigg\}. \quad (13)$$

The fitting coefficients $A_i^{(l)}$ and $\alpha_i^{(l)}$ are taken from work [22]. For estimation of our own energy values QL-method was used.

Distribution of $\rho(\mathbf{r})$ was evaluated from the expression:

$$\rho(\mathbf{r})=\frac{2e}{\Omega|C_0|^2}\sum_{i=1}^{M}\gamma_i\sum_{n=1}^{N_{vz}}\left|\sum_m U_{nk}\sum_{R\in G_0}\exp\left(-iR\mathbf{G}_m(\mathbf{r}-\tau_R)\right)\right|^2, \quad (14)$$

where M is number of the summation points within the Brillouin zone, γ_i is weight components, $N_{vz}=0\cdot\sum_\alpha Z_\alpha N_\alpha$ is effective electron density, Z_α is effective charge of atom, N_α is number of electrons in α-type atom, τ_R is translation vectors.

The self-consistency procedure was reached by the iteration method. The "starting" Hamiltonian was constructed in the approximation of Thomas-Fermi screening that enabled us to avoid mistakes in determining the electron density distribution. The self-consistency criterion required that the difference of its two further values should be smaller that the predetermined accuracy $\varepsilon=0.02$ Ry. For $\rho(\mathbf{r})$ evaluation the eigenenergies were estimated in 657 points of the Brillouin zone taking into account the symmetry of its non-reduceable part. For evaluation of the effective mass of electrons and holes the following equation was used:

$$m^*(\mathbf{k}_0)=\left.\frac{h^2}{\partial^2 E(\mathbf{k})/\partial\mathbf{k}^2}\right|_{\mathbf{k}_0} \quad (15)$$

where k is direction near k_0-point of Brillouin zone. The detailed description of the procedure of acceleration of convergency are given in [27]. The self-consistent values of $\rho(\mathbf{r})$ were obtained after about 27 iteration cycles of the self-consistency procedure.

The calculations showed that due to the peculiarities of the long range acting crystal field among equivalent in the meaning of local symmetry of oxygen position in GGG lattice [21] nonequivalent in the energetic meaning positions may be separated, which, however within 0.02 Ry may be divided into three groups. It should be noted that the distance values oxygen-cation in GGG may also be divided into three groups and among the mentioned divisions into groups (by energies and distances) there is a correlation. In the some way the potentials of gallium atom crystalline surrounding are divided into two groups (Ga in octahedron or in tetrahedron) and for gadolinium atoms within the accuracy limit ε there is only one position.

In Table 1 there are given some of the data obtained as a result of calculations — values of chemical bond energies, degrees of their ionnicity, GGG atoms effective radii.

4.2. Calculation of defect parameters and their concentrations under the influence of irradiation

The self-consistent calculation of ED distribution in the region of the crystal with the distortions of translation symmetry allowed to find out the most probable defect configurations in GGG and mechanisms of their formation by the method of ED space minimization in case of atom shift from its regular site and its migration through quasiequilibrium positions in the adjoining intersites [18]. It was assumed that the rest surrounding atoms remain at their sites (frozen matrix model). At the same time the potential barrier height dividing these positions was found. Two components were estimated: first, the atoms chemical bonding energy, and second, the potential energy required for overcoming of elastic interatomic interaction. We estimated the second component using a variational procedure to choose the most probable path of displacement of atom to an intersite. It should be noted that we considered only the elastic part of the interaction neglecting anharmonic corrections. Displacement of atom from its site, i.e. from its genetic vacancy was being fulfilled until the energy difference of two neighboring quasi-equilibrium atomic positions became less than 0.02 Ry. The total height of potential barrier estimated in such a way characterizes the threshold energy that should be applied to an atom to form a separated Frenkel pair.

The aforementioned barrier may characterize the threshold energy of an atomic displacement T_d which is a phenomenological parameter of the atomic displacement due to elastic interaction with corpuscular radiation or with secondary particles [28]. Such estimations of the minimum values of T_d for atoms forming gadolinium gallium garnets are listed in Table 1. It is remarkable that, whereas the dominant contribution of T_d (up to 85%) for oxygen atoms is due to the chemical bonding energy, this contribution decreases for heavier atoms to 60% (Table 1).

The results for T_d can be used to estimate the defect concentrations corresponding to various configurations, formed by elastic displacements of atoms in gadolinium gallium garnets due to irradiation of a crystal with different types of radiation. Such estimations were carried out earlier in [15, 29] for various values of T_d within the interval $20\div100$ eV since there were no data on the values of T_d in GGG. However, the formation of defects in the sublattices consisting of different types of atom was considered independently, which is justified only if the radiation does not stimulate branched cascades of atom-atom collisions. For irradiation causing cascades (for example, neutron irradiation), we need to include collisions of different types of atom not only with different masses but also with different values of T_d.

Table 1. Some quantum-chemical parameters of gadolinium-galium garnet single crystals

Type of ion (position)	Effective ionic radius, Å	Chemical bond energy, eV	Thresh, displacement energy, eV
0(I)	1.25	33	38
0(II)	1.23	34.3	40.5
0(III)	1.23	34.6	41.2
Ga^{3+}(oct)	0.81	37.7	56
Gd^{3+}	1.31	40.1	75.7

Chemical bond	Degree of ionicity of chemical bond
$[Ga-0(1)]_{tetr}$	0.64
$[Ga-0(2)]_{oct}$	0.60
$[Ga-0(13]_{oct}$	0.77

Table 2. Concentration of displacement defects n_d (cm^{-3}) in gadolinium gallium garnet sublattices after irradiation with a unit dose (1 cm^{-2}) of electrons and neutrons

Type of trradition	Energy, MeV	n_d in sublattice		
		Gd	Ga	O
Electrons	1.25	0.0006	0.0992	0.493
	3.5	0.416	0.577	0.779
Neutrons	2	2.15	2.67	9.24

The total concentration of displacements in the sublattice of atoms of type j can be expressed, as in [29], in the form

$$n_{d_j} = n \cdot \Phi \cdot \sum_i \int_{T_{d_j}}^{T_{m_i}} \frac{\partial \sigma_i(E, T_i)}{\partial T_i} \nu_{ij}(T_i)\, dT_i, \qquad (16)$$

where Φ is the fluence of radiation particles; n is the density of atoms in the crystal; $\partial\sigma_i/\partial T_i$ is the differential crosssection for the displacement of the primary knocked-out i-atom; T_i is the recoil energy of the primary knocked-out atom; T_m is the maximum possible recoil energy; $\nu_{ij}(T_i)$ is the number of displaced atoms of type j per single knocked-out i-type atom with energy T_i. It is assumed that an atom with a recoil energy $T < T_d$ is not displaced at all, but in the case of an atom with an energy $T > T_d$ the probability of displacement is 1. The differential cross section of the displacement process is then equal to the cross section of energy transfer to the atom within the limits T_d and T_m. In the case of electrons in the Coulomb field of a nucleus takes place and an expression for $\partial\sigma/\partial T$ is then given in the relativistic case by the McKinley-Feshbach formula [30]. Neutron scattering is usually described as scattering of solid spheres [31], which determines the appropriate expression for $\partial\sigma/\partial T$ in this case.

We calculated the cascade functions $\nu_{ij}(T_i)$ by statistical computer modeling of a cascade of atomic collisions in a triatomic compound. The initial assumptions underlying the cascade model were the following: we assumed that there are only pair atomic collisions, they are mutually independent, and take place as collisions of solid spheres; all the collisions are elastic for $T < T_I$ and for $T > T_I$, the energy is expended only on ionization ($T_i \sim$ A in kilo-electron volts, where A is the atomic mass [31]); the energy of an incident atom is divided between this atom and the atom with which it collides, so that the total kinetic energy of the atoms after collision is equal to the original energy of the incident atom prior to the collision. It is also assumed that each knocked-out atom necessarily collides with one of the atoms forming the gadolinium gallium garnet lattice, but the crystal structure was not taken into account. Under these assumptions, we modeled the randomly developing cascade of atomic displacements in gadolinium gallium garnets. Investigating the energy losses of knocked-out atoms and tracking all the atoms until they come to rest, we counted their number in each sublattice; the cascade was stimulated repeatedly in order to obtain a statistical estimate (between 500 and 5000 times, depending on the energy of the knockedout atoms). Hence, we obtained the cascade functions $\nu_{ij}(T)$ for all atoms in the gadolinium gallium garnet sample and calculated the corresponding concentrations of various defect configurations formed in gadolinium gallium garnets irradiated with high-energy electrons and neutrons (Table 2).

Table 3. A some characteristics of the defect centers

Center type (cond. signes (sites))		Effective charge (e/Ω)	Migration energy (eV)	Annihilation radius (nm)
$A - V_0$	(1)	+1.32	1.86	3.24
$B - V_0+e$	(1)	+0.86	2.01	2.36
$C - V_0+2e$	(1)	−0.02	2.43	1.64
$D - V_0$	(2)	+1.37	1.74	3.59
$E - V_0+e$	(2)	+0.79	1.95	2.51
$F - V_0+2e$	(2)	+0.13	2.36	1.97
$G - V_0$	(3)	+1.40	1.67	3.78
$H - V_0+e$	(3)	+0.76	1.84	3.31
$I - V_0+2e$	(3)	−0.14	2.12	2.14
$J - V_{Ga}$	(tet)	−2.89	1.34	4.12
$K - V_{Ga}+p$	(tet)	−1.16	1.57	3.81
$L - V_{Ga}$	(oct)	−3.12	1.45	3.98
$M - V_{Ga}+p$	(oct)	−1.43	1.67	3.57
$N - V_{Gd}$		−1.78	1.12	4.32
$O - V_{Gd}+p$		−1.12	1.56	3.82
$P - Gd_{(as)}$		−2.07	1.06	–
$Q - Gd_{(as)}+p$		−1.06	1.45	–

Calculations, accordingly to the scheme described in chapter 4.1 for the single defect centers enabled us to determine such their parameters as the effective charge, migration energy, annihilation radius. There were considered the following types of defect centers: oxygen vacancies V_0; the vacancies, trapping one or two electrons V_0+e (F^+) and V_0+2e (F) respectively; gallium and gadolinium vacancies the free ones V_{Ga}, V_{Gd} and those trapping holes $V_{Ga}+p$ and $V_{Gd}+p$, as well as the so called anti-site gadolinium defects (gadolinium ions that are in octahedric gallium positions) which accordingly to [14] may be found in GGG crystal in rather a large number. The results of these calculations are given in Table 3.

4.3. Calculation of spectroscopic parameters of optical transitions with the defect centers participation

Formation of vacancies in the regular lattice sites causes appearance of local potential which promotes emergence of localized levels formed by splitting from the permitted energetic bands of the crystals. Green functions method was used for evaluation of eigen energies and crystal wave functions of the vacancies. On the base of these results the energies and probabilities of optical transitions including the defect centers levels were estimated. There were considered the same centers as those in chapter 4.2. In the calculation there were taken into account only transition from the filled states in the unfilled ones.

The calculation technique is described in details in [32]. The summing up of the values of wave function vacancies was done in more than 4500 points of the non-reduceable part of Brillioiun band. The parameters of phonon spectra of GGG that were necessary for estimation of the lattice dynamics were taken from the work [33].

The obtained spectroscopic characteristics of the optical transitions "valence band – vacancy centre", placed into UV and the visible range of spectrum are given in Table 4, and the diagrams of the corresponding transitions are shown in Fig. 18.

These spectroscopic parameters in the principle allows us to make the AA spectra approximation of the GGG irradiated crystals with a set of Lorentian shape lines corresponding to optical transitions with participation of defect centers. In [32] we made an attempt to approximate the AA spectra induced in GGG by electron irradiation of $E=1.3$ MeV energy of $\Phi=10^{17}$ cm^{-2} fluence, and also with electrons of $E=3.5$ MeV and $\Phi=10^{17}$ cm^{-2}. The first spectrum according to experimental results (see chapter 3) is caused by ionizing recharging processes and in the formation of the second one the true radiation defects take part. The approximation was done by the method of linear regression. The variations of correspondent

Table 4. Spectroscopic characteristics of optical transitions "valence band-center" for different vacancy type centers in GGG crystal (E – the transition energy, P and ΔE – intensity and width of the transition of the middle of the hight respectively, f – the oscillator force)

Center type (cond. signes (sites))		E, eV	ΔE, eV	P, arb. un.	f, arb. un.
$A - V_0$	(1)	2.31	0.37	0.49	0.1813
$B - V_0+e$	(1)	3.5	0.37	0.53	0.1961
$C - V_0+2e$	(1)	3.47	0.37	0.46	0.1702
$D - V_0$	(2)	1.79	0.31	0.39	0.1209
$E - V_0+e$	(2)	2.90	0.31	0.43	0.1333
$F - V_0+2e$	(2)	3.01	0.31	0.36	0.1116
$G - V_0$	(3)	1.01	0.25	0.21	0.0525
$H - V_0+e$	(3)	2.16	0.24	0.16	0.0384
$I - V_0+2e$	(3)	2.23	0.24	0.17	0.0408
$J - V_{Ga}$	(tet)	4.62	0.31	0.17	0.0527
$K - V_{Ga}+p$	(tet)	4.47	0.16	0.23	0.0368
$L - V_{Ga}$	(oct)	4.19	0.27	0.22	0.0594
$M - V_{Ga}+p$	(oct)	3.00	0.19	0.21	0.0399
$N - V_{Gd}$		5.62	0.14	0.08	0.0112
$O - V_{Gd}+p$		5.38	0.19	0.02	0.0038
$P - Gd_{(as)}$		5.74	0.09	0.04	0.0036
$Q - Gd_{(as)}$		5.16	0.11	0.04	0.0044

centers concentration were taken as the parameters of the regression which was estimated by the intensity of components of the absorption spectrum lines accordingly to the Smakula-Dexter formula [34]. While making approximation of the second spectrum the data on the concentration of the radiation defect displacement were taken into account (see above).

The results of the first spectrum approximation reveal two clear tendencies of reciprocal transformation of defect centers in the result of the ionization recharge increase of F-centers and cation centers concentrations. For the second spectrum there was also noted increase of F^+ – and V_{Ga}-centers, but to a great extend due to formation of new the other radiation defects. The B-band is probably caused by the oxygen centers, while the formation of the A band, as well as the change of the spectrum near the absorption edge is mainly caused by the cation defects.

5. Discussion

A transient absorption in GGG crystals is evidently of the same nature as that of YAG crystals [3] and is caused by formation of unstable at RT colour centers that are connected with the both electron excitations – the auto-localized ones and those localized at undeep levels of trapping near the defects and impurities. Decay of such centers lasts for a period shorter than 10 sec [35]. During this process there may appear luminescence in the band 32000–36000 cm^{-1} or stable colour centers may be formed

The experimental data presented in chapter 3 as well as the results of the works [7, 10, 11] show that at the absorbed doses up to 10^7 Gy the stable at room temperature additional absorption does not depend upon the type and radiation energy (UV-light, γ-quanta, electrons of energy up to 3.5 MeV). Its dose dependence is characterized by the tendency to saturation (Fig. 9). The complete destruction of AA takes place after annealing of the irradiated samples at $T > 450$ K. These facts allow us to connect A and B bands with the ionization recharge of genetic defects (their concentration, as it was indicated above, may reach 10^{19} cm^{-3}) [13]. From the analysis of temperature dependences of the additional absorption destruction and thermo-stimulated processes in irradiated crystals (Fig. 10) it may be concluded that AA is formed by at least two types of CC. The decrease of thermoelectromotive force in the region 340 K testifies about the appearance of a non-compensated positive charge during the destruction of A – band, and increase of thermo-electromotive force in the region of 410 K is caused by release of the negative charge during of the B-band destruction.

Taking into account the obtained results and also the known data about the characteristics of AA in the other rearearth gallium garnets ($Nd_3Ga_5O_{12}$, $Sm_3Ga_5O_{12}$) [4,11] it is possible to assume that the appearing CC are connected with the ionization recharge of genetic defects being typical for GGG structure: A – band is caused by trapping of the hole by a cation sub-lattice defect (most probably Ga vacancy or Gd ion in octahedral coordination), B-band is connected with the absorption of F-type centers. We shall call them *the ionization colour centres*.

Thus, it is possible to confirm that the state of the defect subsystem of as-grown crystal determines the nature of the formed during irradiation defects, peculiarities of their manifestation in optical properties as well as running of other processes with the nonequilibrium charge carriers participation. As a proof of it one may use data about the radiation-induced optical properties of GGG with various impurities making a significant influence on the defect subsystem state of as-grown crystal. In particular, doping of izovalent In^{3+}, Sc^{3+}, Nd^{3+} ions does not change the character of absorption spectra of ionization defects but only increases its intensity. Probably, the presence of such impurities stimulates an increase of content of genetic defects in the crystal.

The Fe and Cr impurity ions, which as a rule are in the structure in three valent state, being introduced into the crystal can easily change a valency at external influence and compete with genetic defects in trapping of by irradiation generated charge carriers and cause the changes of relative A and B bands intensity and appearance of new bands in the AA spectrum (Fig. 8, see also [36]).

The GGG structure doping of the Me^{2+} (Ca^{2+}, Mg^{2+}) nonizovalent ions in the concentrations, that exceed the necessary for compensation of the charge of uncontrolled Me^{4+} impurities, changes significantly the state of crystal defect subsystem. In this case non typical for nominally pure GGG crystals complex defects $[F^+Me^{2+}]$ are formed. Their appearance causes the change of character of radiation crystal colouring.

Peculiarities of photo- and gamma-induced transformations of GGG-Ca(Mg) (Fig. 11) including CCC $[Me^{2+}F^+]$ may be explained in the following way. Studying of the photoconductivity spectra did not find out any photocurrent maxima in the range of CCC absorption, while a photocurrent in the range of 23000 cm^{-1} in irradiated crystals was found [16, 37]. It enables us to assume that absorption in the range of 29000 cm^{-1} is caused by intracenter transition between the ground state and excited one of CCC (Fig. 19). After this a part of centers relaxes to the ground state and the rest ones have probably a possibility (for explanation of photochromic properties of the crystal) of tunnelling of electrons from excited state of CCC to a level of another defect (most probably of the oxygen sublattice) and formation of F-type center. In such a case any radiation- or photo-induced absorption band at 23000 cm^{-1} corresponds to the optical excitation of electron from F-center to the conduction band that is being accompanied with photoconductivity in that spectral region. The ionized CCC causes an appearance of absorption in the range $\nu > 37000$ cm^{-1}.

A good correlation of photoinduced band 23000 cm^{-1} with of the B band spectral position and its temperature destruction of irradiated by gamma-quanta and electrons of nominally pure GGG crystals (Fig. 8) testifies that the long-wave maximum of GGG-Me^{2+} additional absorption is connected with F-type centers.

Simultaneous running of the two processes (relaxation and tunnelling) explains rather an insignificant clearing at the band 29000 cm^{-1} (the absorption coefficient decreases no less than for 10%) even in case of long periods of irradiation.

In case of irradiation with the light of argon laser or at heating of the crystal electrons are released from the levels of F-type centers and get into the conduction band and than they are being trapped by the ionized CCC reestablishing in such a way the original charge state of defects.

In case of irradiation with doses more than 10^7 Gy with high-energy electrons (3.5 MeV) as well as in case of irradiation with fluxes of protons and neutrons ($\Phi_n > 10^{13}$ cm^{-2}) a large number of new defects is formed in GGG crystals that are crea ted accordingly to the impact mechanism and we will call them *the radiation defects*. The C-band is connected with the radiation CC that is supported by absence of the tendency to saturation of dose dependency of its intensity as well as high

temperatures of its destruction (Fig. 13, 14). Accordingly to the calculations of radiation defect concentrations (see Table 2) the most effective radiation defect formation takes place in oxygen sublattice at highenergy electron and neutron irradiation. Therefore it is possible to assume that C-band is formed in main by F-type CC or more complex defects that include a vacancy of oxygen. The difference of spectroscopic parameters of F-type centers formed in the result of ionization recharge of genetic defects and due to atom displacements accordingly to the impact mechanism may be most probably caused by the differences of the forms of their stabilization in the process of the crystal synthesis (for ionization CC) and impact displacement (for radiation CC).

Formation of radiation defects in the GGG structure causes the appearance of luminescence with the maximum at 19000 cm^{-1} (Fig. 15) which has the recombination nature and the radiation defects serve as the centers of recombination [38].

Of peculiar interest are the changes taking place under the influence of ionizing irradiation in the spectral region near the fundamental absorption edge of GGG crystals. These changes clearly demonstrate the action of different mechanisms of defect formation. In case of use of small doses of gammaand electron irradiation the clearing of crystal near the edge of fundamental absorption takes place, i.e. a part of genetic defects contributing to the absorption in the range $44000 \sim 33000$ cm^{-1} changes their charge state, stops absorbing light in the given region and forms CC corresponding to A and B additional absorption bands. With the increase of the absorbed dose of electron irradiation in case of irradiation with neutrons and ions the transparency of GGG near the edge decreases and the fundamental absorption edge becomes wider.

In Fig. 20 there is shown the dependence of the position of the edge of the fundamental absorption (E_k) versus the particle fluence. For the value characterizing the position of the edge a wave number at which the absorption coefficient was 10^2 cm^{-1} (in case of electron and neutron irradiation) and about 10^4 cm^{-1} (in case of ion implantation) is taken. If we assume that darkening in the region of the fundamental absorption edge is proportional to the number of defects causing the spreading of the bands then the slope of dose dependences determines a value $\partial n_d/\partial \Phi$ which characterizes defect formation efficiency at various kinds of irradiation. It is seen from the figure that the radiation defect for mation takes place most efficiently at cascadeforming irradiation – neutron and Ne^+ ion fluxes. In this case accumulation of point defects (e.g. $[V_0 V_{Ga}]$ associants) and the whole disordered regions may be formed [39].

In case of the vacancy type defects formation some energy levels splitted from the permitted bands in the result of local distortion of the crystal structure appear in the band gap.

Theoretically calculated positions of such levels caused by the presence of various vacancy types as well as their spectroscopic characteristics are presented in Table 4. Comparison of energy positions of the levels with the spectra of additional absorptions shows that in the region of the A, B, C absorption bands there are levels of vacancy type in sublattices of oxygen and gallium. The defects of gadolinium sublattice have their levels near the conduction band. Optical transitions to the levels of vacancy defects can make a certain contribution into the AA spectrum and be one of the reasons that it is more complicated.

It should be mentioned, however, that these defects will also have intracenter levels caused by influence of crystal field on the defect (ground and excited levels of defect) that will cause complication of energy diagram of the crystal with defects. Probably, just these intracenter levels determine the character of AA spectrum. Calculation of spectroscopic parameters of intracenter transitions is a special task and it will be considered in an another article.

6. Conclusions

Thus, the radiation stimulated changes of GGG crystal properties are determined by the running of two main processes: ionization recharge of genetic defects and radiation defect formation accordingly to the impact mechanism.

The first process prevails in case of gammaand electron irradiation at absorbed doses up to 10^7 Gy. In this case value and character of induced changes are determined by the state of crystal defect sub-system. Experimental results show that while making influence on defect sub-system (change of the growth conditions, thermo-treatment, doping of impurity ions) it is possible to a certain degree to control the process of CC ionization formation achieving the decrease of crystal degradation degree under the irradiation.

The second process prevails at large doses (more than 10^7 Gy) of high-energy electron irradiation, irradiation with neutrons, protons and ions. Efficiency of radiation defect formation increases with the rise of the particles energy and mass. Theoretical studying allowed to calculate for the first time the displacement threshold energies of atoms in GGG and taking into account their values to estimate the radiation defect concentrations.

The rigorous theoretical calculations combined with phenomenological conceptions allowed to obtain some parameters of point defects in GGG crystals which can be used for clearing up their nature and interpretation of experimental data. Such a comprehensive approach is, in our opinion, the most perspective one for further investigations of own and radiation-induced defects in GGG.

The authors are thankful for assistance in making experimental results and useful discussions to our colleagues I. Bolesta, V. Vasyltsiv, Ya. Dovgyi, Ya. Zakharko, I. Savitsky, U. Ulmanis, A. Shakhov.

References

1. *L.G. Karaseva, N.Yu. Konstantinov, V.V. Gromov et al.*: Interrelation between transient color centers creation in laser crystals and their generation properties. Zh. Prikl. Spectr., **45** (1986) p. 205 (in Russian).
2. *K. Yoshida, H. Yoshida, Y. Kato.*: Characterisation of high average power Nd:GGG slab lasers. IEEE J. Quantum Electron., **QE-24** (1988) p. 1188.
3. *A.O. Matkovskii, D.Yu. Sugak*: Color centers in garnet single crystals. Yttrium aluminium garnet. Mineralog. Sbornik, **41** (1987) p. 21 (in Russian).
4. *A.O. Matkovskii, D.Yu. Sugak, I.I. Chegil et al.*: Dopants influence on the spectroscopical properties of rare-earth gallium garnets. Mineralog. Sbornik, **43** (1989) p. 38 (in Russian).
5. *G.J. Pogatshnik, L.S. Cain, Y. Chen, B.D. Evans*: Optical properties of colour centers in calcium-stabilized gadolinium gallium garnet. Phys. Rev., **B43** (1991) p. 1787.
6. *M. Pardavi-Horvath, M. Osvay*: Thermoluminescent properties of gadolinium garnet crystals containing Ca^{2+} impurity. Phys. Stat. Sol., **A80** (1983) p. 183.
7. *L. Zhang, C. Lin, H. Liu et al.*: Investigation of color centers in doped GGG crystals. J. Chin. Silic. Soc., **11** (1983) p. 399 (in Chinese).
8. *A.O. Matkovskii*: Radiation-stimulated processes in inorganic materials for information processing systems. Izv. Acad. Nauk Latv. SSR, Ser. fiz.-techn. nauk, **3** (1990) p. 79 (in Russian).
9. *A.O. Matkovskii, D.Yu. Sugak, S.B. Ubizskii et al.*: Radiation – stimulated processes in gadolinium gallium garnet single crystals. Phys. Stat. Sol., **A128** (1991) p. 21.
10. *M.Kh. Ashurov, I.N. Nasyrov, V.V. Osiko, P.K. Khabibullaev*: GSGG crystals clearing in UV region after gamma-irradiation. Zhurnal Prikl. Spectr., **48** (1988) p. 124.
11. *A.E. Nosenko, L.V.Kostyk*: Radiation color centers in gallium garnets. Ukr. Fiz. Zhurnal, **31** (1986) p. 75 (in Russian).
12. *S. Geller*: Crystal chemistry of the garnet. Zeitschrift fur Kristallographic, **B125** (1967) p. 1.
13. *G.M. Kuzmicheva, S.N. Kozlikin, E.V. Zharikov et al.*: Point defects in gadolinium gallium garnet. Zhurnal Neorg. Khimii, **33** (1988) p. 2200 (in Russian).
14. Elements and devices on bubble domains. Handbook. Ed. N.N. Evtikhiev and B.N. Naumov: Radio i Svyaz, Moscow 1987 (in Russian).
15. *A.O. Matkovskii, D.Yu. Sugak, S.B. Ubizskii et al.*: Effect of ionizing radiation on the electronic technic materials. Svit, Lviv 1994 (in Russian).
16. *A.O. Matkovskii, D.Yu. Sugak, I.M. Bolesta et al.*: Photochromic properties of gadolinium gallium garnet contained Ca and Mg ions. Zh. Prikl. Spectr., **51** (1989) p. 542 (in Russian).
17. *E.D. Aluker, D. Yu. Lusis, S.A. Chernov*: Electron excitation and radioluminescence of alkali-halides crystals. Zinatne, Riga 1979 (in Russian).

18. *Ya. O. Dovgy, I.V. Kityk, A.O. Matkovskii et al.*: Quantum – chemical approach to defect states creation in gadolinium gallium garnet. Fiz. Tverd. Tela, **34** (1992) p. 1078 (in Russian).
19. *A.I. Kuznetsov, B.R. Namozov, V.V. Murk*: Relaxed electron excitations in Al_2O_3, $Y_3Al_5O_{12}$ and $YAlO_3$. Fiz. Tverd. Tela, **27** (1985) p. 3030 (in Russian).
20. *P. Bak*: Electronic band energy calculations. Sony Brothers, New York 1993.
21. *Landolt-Bornstein*: Zahlenwerte und Funktionen aus Naturwissenschaft und Technik. Neue Serie. Gruppe III: Kristall und Festkörperphysik, V. 12. Berlin, 1972.
22. *G.B. Bachelet, D.R. Haman, M. Shluter*: Pseudopotentials that works: from H to Pu. Phys. Rev., **B26** (1982) p. 4199. 23. J. Slater: Quantum chemistry. Benjamin Press, Nev York 1977.
23. *J. Slater*: Quantum chemistry. Benjamin Press, Nev York 1977.
24. *M.I. Kolinko, I.V. Kityk, A.S. Krochuk*: Band Energy Parameters and Condensity Functions of the orthorombic KI. J. Phys. Chem. Sol., **53** (1992) p. 1315–1320.
25. *W. Kohn, L.J. Scham*: Selfconsistent equations including exchange and correlation effects. Phys. Rev., **140,** no. 3 (1965) p. 1133.
26. *V.V. Kudriavtsev*: Integrals and series. Nauka, Moscow 1984.
27. *Ya. O. Dovgy, M.K. Zamorskii, I.V. Kityk, N.I. Kolinko*: Preprint ITF-89-19R. ITF AN USSR, Kiev 1989.
28. *M. Thompson*: Defects and radiation damages in metals. Mir, Moscow 1971 (in Russian).
29. *S.B. Ubizskii, A.O. Matkovskii, D. Yu. Sugak et al.*: Radiation defects in $A_3B_5O_{12}$ and ABO_3 oxides. Izv. Acad. Nauk Latv. SSR, Ser. fiz.-techn. nauk, **6** (1989) p. 12 (in Russian).
30. *W.A. McKinley, H. Feshbach*: Coloumb scattering of relativistic electrons by nuclei. Phys. Rev., **74** (1948) p. 1759.
31. Point defects in solids. Ed. B.I. Boltax, T.V. Mashovets, A.N. Orlov. Mir, Moscow 1979 (in Russian).
32. *Ya. O. Dovgy, I.V.Kityk, A.O.Matkovskii et al.*: Spectroscopical parameters of color centers in $Gd_3Ga_5O_{12}$ single crystals. Fiz. Tverd. Tela, **35** (1993) p. 290 (in Russian).
33. *A.I. Bilyj*: Doctors Thesis. Lviv University, 1986.
34. *D.L. Dexter*: Absorption of light by atoms in solids. Phys. Rev., **101** (1956) p. 48.
35. *D.Yu. Sugak, A.O. Matkovskii, I.M. Solskii et al.*: Transient luminescence and transient absorption in GGG single crystals. Intern. Conf. on Luminescence, Storrs, USA 1993, p. Th4-92.
36. *M. Kh. Ashurov, E.V. Zharikov, V.V. Laptev et al.*: Influence of chromium ions on color centers formation in crystals with garnet structure. Dokl. Acad. Nauk SSSR, **282** (1985) p. 1104 (in Russian).
37. *A.O. Matkovskii, D.Y. Sugak, I.M. Bolesta, I.V. Savitskii*: Mechanism of photogeneration of carriers in gadolinium gallium garnet crystals. Fiz. Tverd. Tela, **33** (1991) p. 3091.
38. *V.I. Vasyltsiv, Ya. M. Zakharko, A.O. Matkovskii et al.*: Luminescence and photoconductivity of gadolinium gallium garnet single crystals irradiated by high-energy electrons and neutrons. Phys. Stat. Sol., **A140** (1993) p. 353.
39. *S.B. Ubizskii, A.O. Matkovskii, R.M. Kholyavka, M.M. Rak*: Investigation of radiation-stimulated processes in epitaxial yttrium-iron garnet films. J. Magn. and Magn. Mater., **125** (1993) p. 110.